preparation for advanced functional surfaces, on-line quality detection and automatic control of laser processing, and laser direct manufacturing of metal parts based on precise laser cladding.

Fig. 10 shows the precise and flexible AM of a W/Ni alloy component for a hard X-ray telescope collimator with laser cladding for use in outer space[24]. This work entailed the employment of parts with the characteristics of overlap multipass laser cladding of tungsten or tungsten/nickel alloys, followed by analyses of the microstructure and composition of the parts. The laser AM system is composed of a 3 kW fast axial flow CO_2 laser, a CNC-controlled working table, a newly developed computer-controlled powder feeder, and a patent coaxial nozzle. An infrared double wavelength thermometer was used to detect the temperature of the melt pool during the process.

Fig. 10 AM process based on high-energy laser beams

3.7 Electron Beam Selective Melting (EBSM) system

The electron beam selective melting (EBSM) system deals with the direct manufacturing of

Fig. 11 The EBSM 250 in Tsinghua.

metallic parts. Parts manufactured by EBSM have been applied in the fields of medicine, defense, and aeronautics, etc. The EBSM system was established in 2004 in Tsinghua (Fig. 11). Because the electron beam had a relatively large deflection error and the manufacturing precision was lower, a digitized control system was developed[25].

A four-channel, high-speed arbitrary waveform generator was developed, as well as digitized automatic moving software for deflection error correction and dynamic focus control. To improve the deflection accuracy, the non-linear magnetic deflection was analyzed. Experiments proved that such a digitized error correction method could greatly improve the precision of deflection precision and reduce the degree of pincushion distortion.

3.8 Laser-guided direct transportation equipment

Laser-guided direct transportation (LGDT) technology applies optical forces to capture, transport, and deposit single-material particles for the fabrication of structures. Taking various types of particles, including living cells, as manipulable engineered materials, it can act as a new enabling technology for use in rapid prototyping manufacturing systems. Applications can be seen in the fields of microfabrication and tissue engineering. LGDT equipment was installed in our lab and applications for AM were created. Considering the relevant practical influences, experiments and numerical simulations were conducted to investigate the conditions and the rules governing the motions of suspended particles during their transportation. The effects and the mechanisms of those influences were also examined. The guidance and deposition of several types of micron-sized particles, such as polystyrenes, were carried out to learn basic operational and measurement skills, as well as to obtain the essential process parameters (Fig. 12)[26].

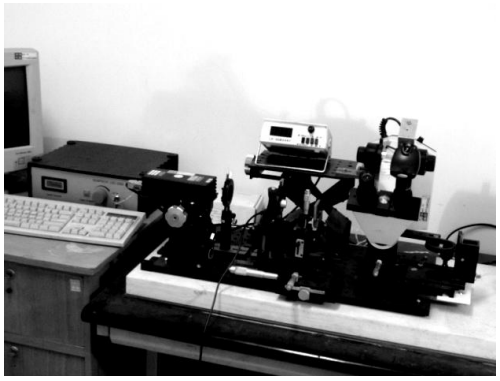

Fig.12 Laser-guided direct transportation system

The driving forces and influences during transportation were discussed next. Based on scattering theory, a computing program was designed that could calculate optical forces precisely. As a result, the distribution of optical forces could be described, giving rise to the conclusion that it is mainly influenced by the optical intensity. The most influential factor during the transportation process is the convection of the suspending medium caused by light absorption. The velocity of the convection can be estimated by a natural convection FEM in an enclosed chamber with an internal heat source. The relevant influential factors were also discussed.

The transportation parameters were discussed in terms of the experimental results and

motion simulations. The offset between the particle stream and the optical axis is determined by the change in the equilibrium position of the optical gradient forces, which is itself caused by transverse influences. In addition, the transport velocity of the particles is determined by optical pressures. Both are affected by optical parameters and also by convectional influence, which is similar to optical forces. The conclusions of this paper can be used as references for the design of laser-guided direct writing systems and for their application to rapid forming processes.

4. AM systems for BM

The goal of BM, which is an interdisciplinary field of AM and tissue engineering, is to manufacture alternative defective human tissues and/or organs. Flexible AM technology is feasible for the manufacture of accurate artificial non-living alternatives, such as prototypes of needed tissues and organs. Moreover, natural organs are composed of different types of cells (including stem cells) and ECMs, and these cells are present in the space of ECMs with a specific distribution and orientation. Therefore, if AM can directly manipulate the cells and ECMs as forming materials, living alternatives with physiological functions could be created.

4.1 Four types of BM systems

Four types of BM systems have been constructed at the Institute of Bio-manufacturing Engineering, Tsinghua, China (Fig. 13)[27-30]. The fabrication methods for these four systems are based on an AM technology of adopted droplet assembly. The first system is a BM platform similar to the AM experimental platform at low temperatures, and is shown in Fig. 6. Particles of bio-materials and/or cells are deposited as their droplets are transformed from a solid state to a

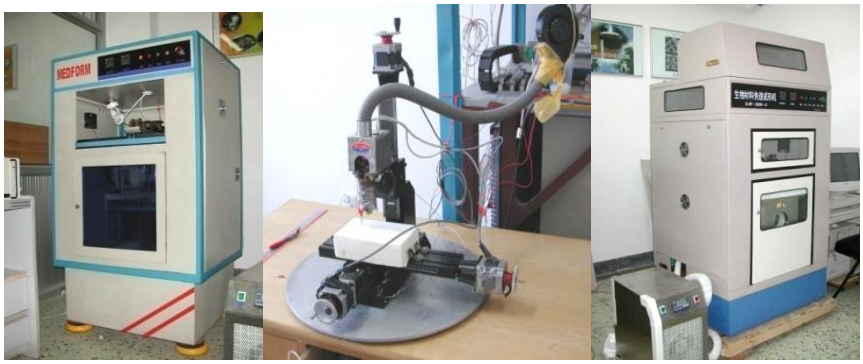

(a) (b) (c)

Fig. 13 Three types of bio-manufacturing systems in Tsinghua
(a) MedForm system for biocompatible materials,
(b) opening bio-manufacturing system, and (c) TissForm system for tissue engineering materials

liquid state. There are many different bio-materials for each of these BM technologies. The MedForm system for biocompatible materials is shown in Fig. 13a. The so-called opening BM

system is shown in Fig. 13b. The TissForm system, which has four nozzles, is shown in Fig. 13c. These types of droplets then solidify and assemble at room temperature or at a low temperature, one by one. Three types of materials for bone tissue engineering scaffolds are provided, and they emerge from three nozzles.

The material slurry is formed into frozen scaffolds in a low-temperature deposition manufacturing (LDM) system, such as the MedForm system, for example. First, the material slurry is fed into the material supply, whose bottom is equipped with a soft pipe connected to a screw pump nozzle. The diameter of the outlet of the nozzle is 0.3 mm. The LDM system builds scaffolds layer by layer and is directly computer-driven by 3D digital models. This is accomplished in a low temperature environment of less than 0 ℃ in the refrigerator. The computer controls the nozzle to move in the X-Y plane, extrude the material slurry, and deposit it onto the platform in the area defined by the digital models. The layer of deposited materials is then frozen on the platform. Also, under the control of the computer, the platform then moves down 0.15 mm in the Z-direction after the forming process of each layer. In this manner, the frozen scaffold is stacked layer by layer.

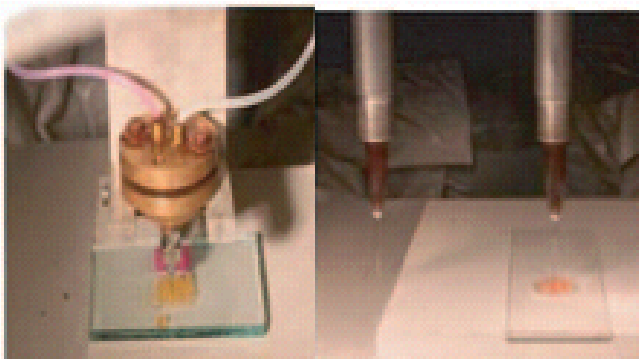

(a) (b)

Fig. 14 Nozzle system in MedForm equipment
(a) Material-mixing single nozzle, and (b) double-nozzle

To ensure the formation of the pores of the vertical cross section, the extruded material is deposited in a series of parallel lines along the Y-direction from the 1st to the 3rd layer, and parallel to the X-direction from the 4th to 6th layer; the scanning direction of the nozzle alternates every three layers. Fig. 14a and b show photos of the single-nozzle and double-nozzle units of the MedForm equipment. The pore dimensions can be adjusted by changing the layer-number interval of the scanning direction and the distance interval of the parallel lines in a single layer. After the forming process, the frozen scaffolds formed by the LDM system are freeze-dried in an ALPHA1-2 Freeze dryer for 38 h to remove the solvent. Following this treatment by freeze drying, the scaffolds remain in the solid state at normal atmospheric temperatures. A quality bio-material system is used in this forming process for bone tissue scaffolds.

4.2 The 3D cell assembler I

Our research group integrated AM technology with a hydrogel solidification process to develop a direct cell-matrix assembly (DCMA) technology[31, 32]. A mixture of high density cells and biocompatible hydrogel materials were chosen as the primary materials, which can be built

layer by layer using a controlled sol-gel phase transition between 0 ℃ and 37 ℃ into a 3D cell-containing structure. DCMA technology can be applied to complex problems that require the arrangement of numerous cell types in the proper 3D structure that can then be induced to generate specific biological functions. One newly developed piece of equipment is the 3D cell assembler I (Fig. 15), with which infant rat cardiac myocytes were used to determine the effectiveness of DCMA.

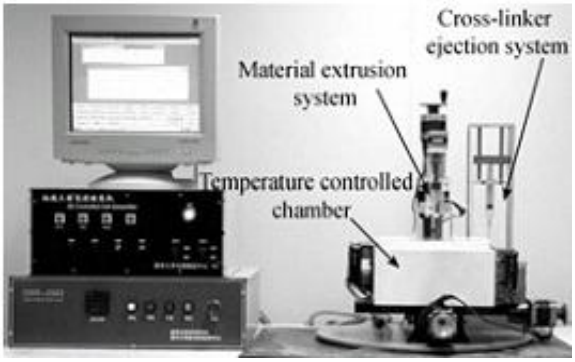

Fig. 15 3D cell assembler I.

Gelatin was dissolved in a hot NaCl (0.15 mol/L, 70 ℃) and Tris-HCl (0.02 mol/L, pH = 7.4) solution to form a 10% (*w/v*) solution that was then filter-sterilized. Sodium alginate was dissolved in a hot NaCl (0.15 mol/L, 70 ℃) and Tris-HCl (0.02 mol/L, pH = 7.4) solution and sterilized twice for 30 min (70 ℃). The solutions were then combined at a 1:1 ratio and mixed thoroughly in a bioclean environment. The isolated cardiac myocytes were mixed into the blended gel at a density of 2×10^8 cells/mL. After thorough mixing, 0.5 mL of the mixture was loaded into a sterilized syringe (1 mL, 0.45 × 16 RW LB). The forming process was carried out following the design structure and programming path at an ambient temperature of less than 10 ℃, using the 3D cell assembler I. The results show that DCMA technology is a promising technology that is currently available to realize the manufacture of complex organs.

4.3 Mechanical stimulation device for AM-BM technologies

The characteristics of the matrix (composition, structure, mechanical properties) and external culture environment (pulsatile perfusion, physical stimulation) of the heart are important characteristics in the engineering of functional myocardial tissue. This study reports on the development of chitosan-collagen scaffolds with micropores and an array of parallel channels (~200 mm in diameter) that were specially designed for cardiac tissue engineering, using a mechanical stimulation device (Fig. 16)[33]. The scaffolds were designed so they would have structural and mechanical properties similar to those of the native heart matrix. Scaffolds were seeded with neonatal rat heart cells and subjected to dynamic tensile stretching using a custom-designed bioreactor. The channels enhanced oxygen transport and facilitated the establishment of cell connections within the construct. The myocardial patches (14 mm in diameter, 1–2 mm thick) consisted of metabolically active cells that began to contract

synchronously after 3 days of culturing. Mechanical stimulation by means of high tensile stress promoted cell alignment, elongation, and the expression of connexin-43(Cx-43). This study confirms the importance of scaffold design and mechanical stimulation in the formation of contractile cardiac constructs.

Fig. 16 shows the scaffold and bioreactor design of myocardium cell assembly. Fig. 16A schematically shows the production of a chitosan-collagen channeled scaffold. Polydimethylsiloxane (PDMS) solution was poured onto a laser-cut acrylite disk with vertical channels. After curing at 60 ℃ for 4 h, the PDMS molds were peeled off the acrylite surface and

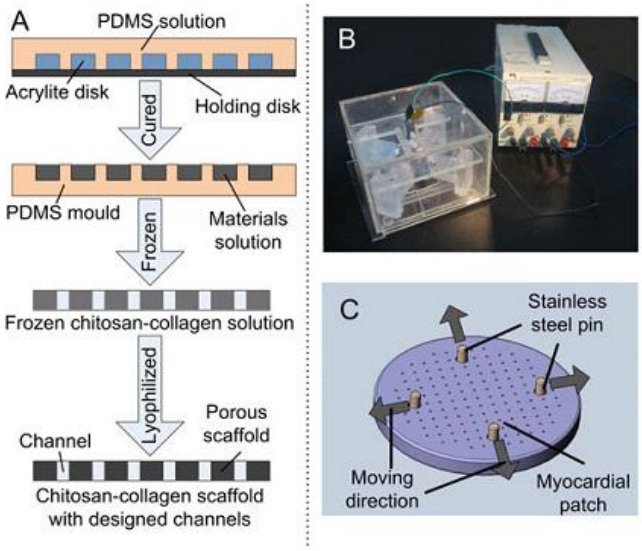

Fig.16 Scaffold and bioreactor design for myocardium cell assembly.

achitosan-collagen solution was poured into the mold. After slow freezing from 4 ℃ to -20 ℃, the sample was removed from the mold and lyophilized to form a porous chitosan-collagen scaffold with an array of channels. A photograph of the mechanical stimulation device, which consists of an adjustable electric source and a chamber, is shown in Fig. 16B. Four sliding blocks are positioned symmetrically inside the chamber to perform back-and-forth movement that is actuated by a motor-controlled cam. Fig. 16C schematically shows the myocardial patches that were installed in the device using four stainless steel pins that were set into four large holes and fixed to each sliding block. The displacement frequency was regulated by the cam geometry and the rotation speed of the motor. The arrows in the figure indicate the directions of the movement of each stainless steel pin.

4.4 New oxidation equipment for the preparation of additive porous anatase titania film

New oxidation equipment, which is presented in a schematic in Fig. 17, is made up of a

high-voltage power supply, a stainless steel electro-bath, a blender, and a cooling system. The stainless electro-bath is used as a cathode at the same time. The cooling system is used to ensure that the temperature of the electrolyte remains constant on the whole. The blender is used to improve the uniformity of the electrolyte[34-36].

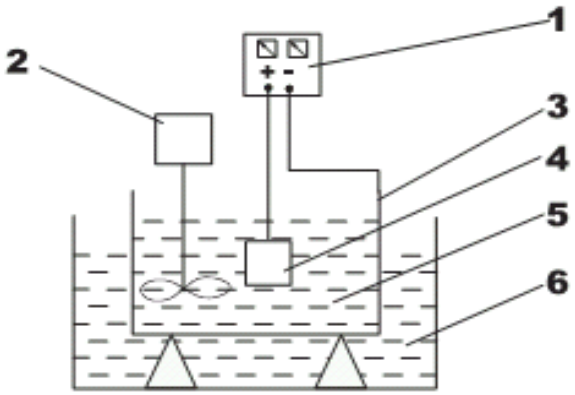

Fig. 17 Sketch of the new oxidation equipment
(1) Power supply, (2) blender, (3) electro-bath-cathode,
(4) titanium plate-anode, (5) electrolyte, (6) cooling water

Porous anatase titanium dioxide with hydroxyapatite coating formed by microarc oxidation (MAO) was made using this equipment. A rectangular Ti grate 1 sample (10 × 10 × 0.4 mm) was used as a substrate. The surfaces of the samples were ground to 1200 grit using silicon carbide sandpaper. This was followed by cleaning with distilled water, acetone, and pickling using a mixture of aqueous HF and HNO_3 acids (with a volume ratio of HF/HNO_3 of 1:3) to remove the native oxide. The samples were then rinsed with distilled water and air-dried prior to pre-anodic oxidation and micro-arc oxidation treatment.

For the pre-anodic oxidation treatment, the pure titanium plate was put into the electrolyte, which was proportioned with 0.05 M oxalic acid and 1000 ml de-ionized water. The titanium plate was the anode and the stainless steel electro-bath was the cathode. The parameters in the pre-oxidation treatment were as follows: the applied voltage was 200 V; the current density was 40 mA/cm^2; the duration was 2 min; a DC power supply was employed in the entire procedure.

Following pre-anodic oxidation treatment, the sample was quickly immersed in the micro-arc oxidation electrolyte, which was composed of 0.02 mol β-glycerophosphate di-sodium penta-hydrate (β-GP), 0.2 mol calcium acetate (CA) and 1000 ml de-ionized water. In the micro-arc anode oxidation treatment, an alternative power supply was used. In the positive section, the processing parameters were: 250 V and a current density of 30 mA/cm^2. In the negative section, the parameters were: 10 V and a current density of 50 mA/cm^2. The processing time for the entire anode oxidation treatment was 10 min, with alternation of the positive and

negative electrode at one-minute intervals.

4.5 Microbead generating device for BM

To engineer tissues with clinically relevant dimensions, one must meet the challenge of rapidly creating functional blood vessels to supply cells with oxygen and nutrients and remove waste products. The physiological diffusion of nutrients within tissue is limited to a distance of approximately 100–200 μm from an adjacent capillary. Distances greater than this result in insufficient oxygen to maintain metabolic functioning. As a result, vascular support of the construct is likely to be one of the most critical factors, if not *the* most critical factor limiting the size, maintenance, and quality of an engineered construct. In addition, adipose tissue is a highly vascular tissue that has a capillary filtration coefficient two to three times higher than that in skeletal muscle. These facts suggest that a rich vascular network is crucial to support the demands of an adipose construct[37, 38].

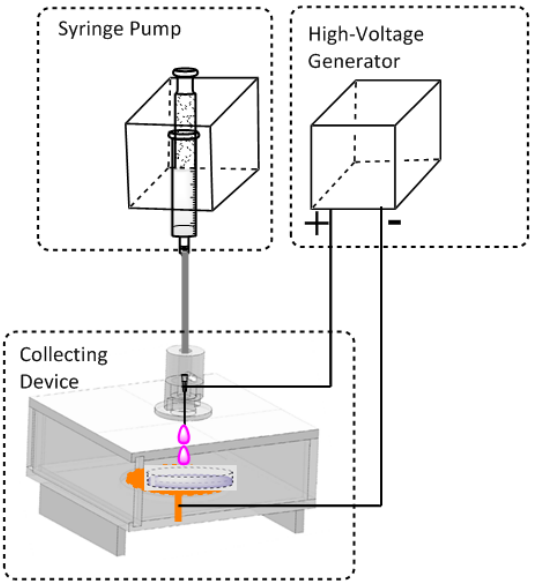

Fig. 18 Schematic of microbead generating device

In brief, the microbead generator is mainly composed of three parts: a syringe pump, a high-voltage power supply, and a collection device, as shown in Fig. 18. The high-voltage field generator (SA167-Y, Tianjin, China) has an AC/DC output voltage ranging from 0 to 40 kV, and the injection pump (TS2-60, Longer Pump Ltd., China) has a promoting speed ranging from 0 to 90 mL/min. The main part of the collection device is a plexiglass box with a pane of sliding glass in the front. A sleeve was set in the center of the upper board, through which a syringe needle and canal were connected to the syringe pump. The sleeve guaranteed perpendicularity, and also facilitated the adjustment of the distance between the needle and the surface of the solidifying solution. A gap was opened in the bottom of the sleeve to facilitate the joining of the positive pole. A copper sheet was inlaid in the center of the bottom board and connected with the negative

electrode from the electrical source. 55 mM calcium chloride ($CaCl_2$) solution was used as a solidifying solution and was placed in a 6 cm^2 glass culture dish above the copper sheet. The alginate/collagen hydrogel solution was extruded through the injection pump at a specific speed. When the electrostatic force and the gravity of the solution became stronger than the surface tension, the solution was dragged such that it formed microdrops that fell into the solidifying solution, where they were converted into insoluble microbeads.

One of the fundamental principles of tissue engineering is sufficient vascularization to supply the growth of newly formed tissue. A pilot study was launched whose aim was to induce adipose formation *in vivo* that had mature vasculature, via the subcutaneous injection of co-culture cell microbeads. The microbeads were composed of alginate and collagen, with differentiated human adipose-derived stem cell (hADSC) distributed evenly inside, and human umbilical vein endothelial cells (HUVEC) attached to the surface on the outside. The channels formed by the gaps among the microbeads provided the space for *in vitro* prevascularization and *in vivo* blood vessel development. The endothelial cell layer outside the microbeads was the starting point of vascular ingrowth. Adipose tissue formation and angiogenesis were assessed for 12 weeks at 4-week intervals. The regenerated vasculature within the transplantation showed functional anastomosis with the host vasculature. A relatively persistent volume and weight of the transplants over time was observed, which indicate that the vasculature formed within the constructs benefited from the formation, maturity, and maintenance of adipose tissue. This method has the potential to provide a microsurgical treatment for adipose regeneration.

5. Software and calculation technology in AM

In modern manufacturing technologies, the manufacturing process is usually composed of an information process and a physical process. The application of computer technology in the manufacturing industry has already help realized a digital description of the information process and has strengthened the coordination between the information process and the physical process. This development has resulted in numerical controlled (NC) design and manufacturing, such as computer numerical control processing technology, flexible manufacturing systems, and computer-integrated manufacturing systems (CIMS). Our lab is one division of the national engineering research center of CIMS. This means that study, education, and research in the fields of software and calculation technology are very important to us.

NC design and manufacturing has only achieved a digital information process and the numerical controlling of tools in the forming process. The transfer of forming materials in a physical process is still completely passive, and is not numerically controlled. Unlike NC technology, however, AM technology has realized not only a digital information process, but a digital physical process as well. In AM and BM, the material-transfer process is based on the piling ability of materials. Controlled by digital information, forming materials are added on-demand and are gradually accumulated in the forming area, step by step, to give shape to the

final parts, which further enhances the flexibility of the formation process[39-41].

For BM technology in particular, the forming materials include biodegradable materials and even cells, as living materials. The physical forming process still remains a process of materials undergoing change. The usual modeling methods need to be alternated. According to the levels of application of AM, there are three stages of BM. The first stage is organ prosthesis manufacturing, which can be divided into two classes, according to whether or not the prosthesis will be implanted. The second stage is indirect cell assembly, which refers to a two-step method of fabricating tissue or organs. The third stage is direct cell assembly, which refers to the direct manipulation of cells, biomaterials, and growth factors, and their deposition at a specific spatial site according to a digital model, whose design is based on an anatomical model of an organ or tissue. In all 3D cell assembly technologies such as cell printing (organ printing and bioprinting), 3D photopatterning, laser-guided direct writing, 3D assembly, and 3D direct controlled cell assembly, certain types of thermo-reversible biomaterials such as gelatin, alginate, chitosan, and fibrin can be mixed with cells and can then be extruded into a low-temperature forming chamber to fabricate a living construct.

5.1 Digital models of a hybrid construct for BM

Here, we discuss an example of digital models of a hybrid construct for BM. The liver is a huge chemical plant that plays an important role in metabolic processes. It is composed of two branched vascular networks and numerous hepatic lobules. The blood supply system is quite extensive and important for the liver's functions. Nutrients, including O_2, are transported through dendri-form vascular networks into every part of the liver, whereas wastes, including CO_2, are simultaneously carried out[42, 43]. Fabricated liver analogs must therefore mimic these special characteristics. Figure 19 shows a branched vascular model that was designed in our laboratory. The red tube-like part was predefined as the branched walls of the vascular system, the yellow part was designed to serve as hepatic tissues (Fig. 19d), and the cyan part was used as a covering

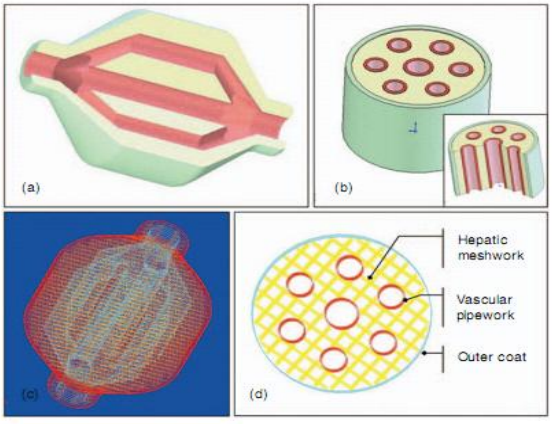

Fig.19 Illustrations of digital models of a hybrid construct for the liver (the red tube lines denote the vascular network; the yellow part is expected to form hepatic tissues)
(a) Cutaway view of the full model with branched network, and one-way inlet and outlet for dynamic perfusion culture; (b) cross-sections of the middle part of (a); (c) a CLI result of (a); and (d) a single CLI layer of (b).

for the entire structure (Fig. 19a, b, and d). The one-way inlet and outlet structure was designed to be connected with a bioreactor to provide for *in vitro* dynamic perfusion culture. Using the preprocessing software Aurora (Yinhua, China), the digital model was transferred to a common layer interface (CLI) file for digital-controlled fabrication at a later time. Fig. 19c shows a CLI derived from Fig. 19a and 19d, which are two of the CLI layers derived from Fig. 19b. Except for the round tubes, the yellow part was woven with crossing threads, thereby providing a secondary meshwork or interconnected macro channels for the exchange of nutrients and waste.

5.2 Model of design and control of macro-cellular morphology

Scaffolds are temporary *in vivo*, and they gradually degrade, in a process that is accompanied by bone regeneration. For this reason, complicated bony structures can be simplified for the convenience of the macrocellular morphology, although several basic requirements must still be satisfied. Scaffolds fabricated in our MedForm equipment are all composed of a series of crossing parallel lines (Fig. 20a)[44]. The extruded slurry was deposited along the Y direction from the 1st to 3rd layers, then along the X direction from the 4th to 6th layers. The scanning directions were alternated every three layers, and highly interconnected and crossed macropores were then formed by the intervals among the lines (Fig. 20b), through which cells could enter all over the scaffold. The line width w could be calculated approximately by the nozzle diameter d_N, the layer height Δh, and the slurry's flow-ability.

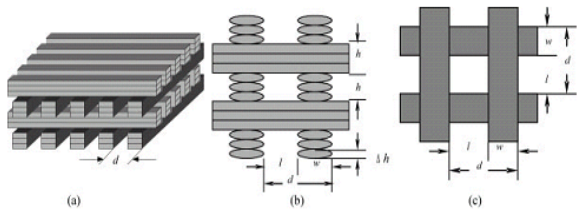

Fig. 20 Megascopic macrocellular morphology designed for LDM

5.3 Bone scaffold hierarchical algorithm based on STL data model

On the basis of data models, including stereolithography (STL) and contour layer interface (CLI), a hierarchical algorithm of a bone scaffold was obtained in the fields of AM and BM, and the data structure and class diagram of an extended model from the angle of a prototyping software system could be generated. An STL file integrates many triangular patches and is expressed by three climax coordinates, and four data items of its outward normal vector were introduced. Because an STL data model describes the structure of a single entity and the data information of CLI models of a single entity patch is obtained following the dispersion, it does not include changes in gradient structure and gradient material[45, 46].

We adopted the operating system of Windows XP, and used the development environment of Visual C++ and a 3D graphic software library (Open Graphics Library), independent of the operating system, window system and hardware environment, and developed a data processing

software system. The BM device was used to drive the shaped hardware unit in the prototyping test. Fig. 21 shows the functions of the software structure that were used for fabrication of the bone scaffold. The interface module was used to realize the data input and output, and the user demands could be executed to browse files in different formats. The display module was used to show graphic pictures of opened files and the matrix transformation of models by OpenGL. The support module was used to provide stable prototyping of the supporting frame and reduce the warping of the auxiliary configuration in terms of material properties, strata configurations, quantity scale, and scan ruling. The filling module was used in the process of filling the composite material unit and the construction material unit between the inner and outer contours of the material structure domain. The layering module was used to realize the special information of the supporting frame modeling, and to design and complete the entitative internal structure information, except for simple geometrical coordinate data. The control module was used in the initialization of the numerical control system, and the setting of layering information, path scanning, and processing prototyping.

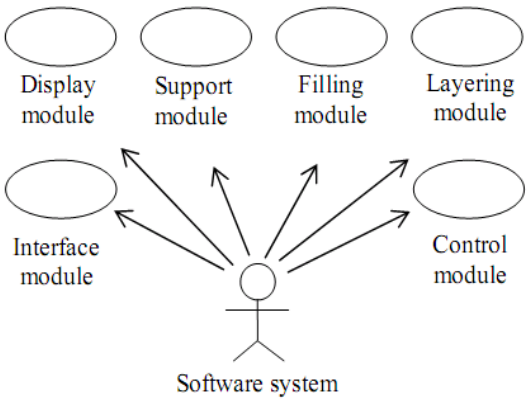

Fig. 21 Functions of the software structure for fabrication of a bone scaffold

Fig. 22 shows the test results. Fig. 22a shows the result for the stratified interface functions of the bone scaffold model; Fig. 22b shows the filling material for the structural fill model. We can ascertain from Fig. 22 that the bone scaffold hierarchical algorithm contains plural property information for bone scaffold materials, multiattribute characteristics of structural changes, and pore structure information of the bone scaffold for tissue engineering, particularly gradient information of composite materials and structures.

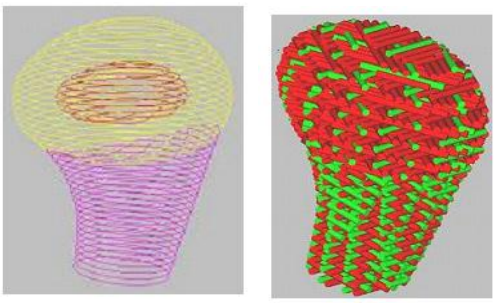

(a) (b)

Fig. 22 The output of structural drawing of bone scaffold model
(a) and illustration of the filling material for structural fill model

In the future, more attention needs to be paid to the integration of data resources, as this will provide us with the essential parameters of AM technologies so that valid data resources, including materials, structures, regions, sprayer, path and filling scan can be established. This could also provide us with the data support that is indispensable for in-depth research in hierarchical algorithms.

6. Conclusions

In conclusion, we would highlight the following points regarding the science and engineering of the AM technologies:

1. Innovative education plays an important role at a high level. Its success depends not only on coursework, but also on experimentation and training opportunities. The four-year undergraduate engineering education should be designed so as to provide students with the knowledge base and intellectual capability to both continue their study and directly engage in practical work. The focus of an undergraduate engineering education should be the development of students as emerging professionals, rather than as fully trained engineers.

2. Because the AM technology has emerging and developing characteristics, it can be readily combined with the study of mathematics, physics, and chemistry, and particularly owing to its relationship with computer engineering, it could be used as a powerful tool for innovative education.

3. More attention must be paid to the construction of the AM and BM laboratory. Though our department has more complete and advanced equipment and devices than it did previously, this significant step forward still constitutes just a first step. A very long road of progress still lies before us. The equipment and devices needed for this progress will need to be designed and fabricated by ourselves.

4. Academic communication on an international level is very important. AM systems can quickly produce models and parts from 3D CAD model data. CT and MRI scan data are obtained from other 3D digitizing systems; the BM technologies were indicated from these data. Using an additive approach to building shapes, the AM and BM systems can combine liquids, powders, sheets, or even living cells to form physical objects. Their most prominent characteristic is their ability to produce real parts from a virtual model.

References

1. DC Li，XY Tian, YX Wang, B H Lu. Development of additive manufacturing technology. Electromachining and Molds, S1. 21, 2012. (in Chinese)

2. YN Yan, SJ Li, RJ Zhang et al. Rapid prototyping and manufacturing technology: principles, representative techniques, applications and developmental trends. In RJ Zhang, eds. Proceedings of the 3rd international conference on rapid prototyping and manufacturing & the 2nd international conference for bio-manufacturing. Beijing, China, p15, 2008. Also J. Tsinghua Science and Technology, 2009, No. S1.1-12, 2009.

3. RJ Zhang,. Editorial: ICRPM-BM 2008 Beijing Conference. Virtual and Physical Prototyping, Vol. 4, No.1, 1, 2009.

4. YN Yan, RJ Zhang et al. Elementary introduction of rapid manufacturing. In YN Yan ed, Proceedings of the 2nd international conference on rapid prototyping & manufacturing 2002, Beijing, China, pp16-26, August 19-20, 2002.

5. YN Yan, RJ Zhang and LF Chen, New Developments in RP and RT in China, in A Special EuroMold 2001 Event, International conference on new developments and trends in RP around the world, Frankfurt/Main, Germany, Nov. 30, 2001.

6. YN Yan, WL Wang, RJ Zhang et al. Rapid Prototyping and Tooling in China. Solid freeform fabrication proceedings, pp873-881, Austin, TX, August 9-11, 1999.

7. YN Yan and J Zhu. Development of rapid prototyping and manufacturing in China. in YN Yan eds. Progress in rapid prototyping manufacturing and rapid tooling, Proceedings of the 1st international conference on rapid prototyping & manufacturing '98, Beijing, China, pp30-38, July 21-23, 1998.

8. YN Yan, RJ Zhang et al, Recent development and trend of rapid tooling technology. in the Proc. of the 1st International conference on Die & Mold Technology, Beijing, China, pp37-51, July 26-28, 2000.

9. QP Lu. Rapid Prototyping Manufacturing Technologies. High Education Press, Beijing, China, 2001. (in Chinese)

10. RJ Zhang et al. Construction and education innovation of series textbooks for engineering materials, The 10th education symposium on engineering materials and basics of material science, Beijing, China, 2005. (in Chinese)

11. RJ Zhang. Practical technologies in advanced formation manufacturing, Tsinghua University Press, Beijing, China, August 2009. (in Chinese)

12. L Liu, Z Xiong, RJ Zhang et al. A novel osteochondral scaffold fabricated via multi-nozzle low-temperature deposition manufacturing. J. Bioactive and compatible polymers

24(5): 146, 2009.

13. Z Xiong, YN Yan, SG Wang, RJ Zhang and C Zhang, Fabrication of porous scaffolds for bone tissue engineering via low-temperature deposition, Scripta Materialia, 46: 771-776, 2002.

14. ZD Shan, YN Yan, RJ Zhang and D Yuan. Rapid substrate manufacturing process from rapid prototyping. In YN Yan ed, Proceedings of the 2nd international conference on rapid prototyping & manufacturing 2002, Beijing, China, pp412-418, Beijing, China, August 19-20, 2002.

15. RJ Zhang et al. Study on scanning process of selective laser sintering (SLS). In YN Yan eds. Progress in rapid prototyping manufacturing and rapid tooling, Proceedings of the 1st international conference on rapid prototyping & manufacturing '98, Beijing, China, pp72-78, July 21-23, 1998.

16. YN Yan, G Zeng, L Wu and RJ Zhang. Study on the key technologies integration of rapid prototyping.. In YN Yan eds. Progress in rapid prototyping manufacturing and rapid tooling, Proceedings of the 1st international conference on rapid prototyping & manufacturing '98, Beijing, China, pp99-110, July 21-23, 1998.

17. C Feng, SJ Yan, RJ Zhang and YN Yan. Heat transfer analysis of rapid ice prototyping process by finite element method, Materials and Design, 28, 921~927, 2007.

18. C Feng, RJ Zhang et al., Rapid prototyping technology of low temperature ice forming, in Proc. of the 8th international conference on rapid prototyping, eds. T. Nakagawa et al., Tokyo, Japan, June 12~13, pp190-194, 2000.

19. SK Chan, YM Zhu RJ Zhang et al. Study on properties and shrinkage of photoresins used in SLA. In YN Yan eds. Progress in rapid prototyping manufacturing and rapid tooling, Proceedings of the 1st international conference on rapid prototyping & manufacturing '98, Beijing, China, pp126-131, July 21-23, 1998.

20. F Liu et al. Application of spraying technology in bio-manufacturing engineering. J. Mechanical Engineering, 42(12): 13~20, 2006. (in Chinese)

21. DZ Wei, RJ Zhan et al. Mathematical model of micro-droplet spraying driven by piezoceramics. China Mechanical Engineering, 16(7): 611-614, 2005. (in Chinese)

22. DZ Wei, RJ Zhan et al. Design of device of micro-droplet spraying by piezoceramics. J. Tsinghua University, 44(8): 1107-1110, 2004. (in Chinese)

23. F Liu. Research of biomaterial micro-deposition manufacturing based on tip-pen direct writing. Ph.D. dissertation, Tsinghua University, Beijing, China, April 2007. (in Chinese)

24. ML Zhong et al. Laser direct manufacturing of tungsten nickel collimation component, J. Materials Processing Technology, 147: 167-173, 2004.

25. J Zhang, F Lin et al. Digitized dynamic focus control in electron beam melting. Proceedings of the international conference on advanced technology of design and manufacture, Beijing, China, pp352-355, Niov.23-25, 2010.

26. LF Chen, YN Yan and RJ Zhang, Effects of convection in laser-guided transportation, J. Mechanical Engineering Science, Vol.218, Part C: 775-782, 2004.

27. TK Cui, YN Yan, RJ Zhang et al. Biomodeling and fabricating of a hybrid PU-collagen nerve regeneration conduit. IEEE International Conference on Virtual Environments,

Human-Computer Interfaces and Measurement Systems, Hong Kong, China, IEEE, May 11~13, 2009

28. TK Cui, YN Yan, RJ Zhang et al. Rapid prototyping of a double-layer polyurethane-collagen conduit for peripheral nerve regeneration. Tissue Engineering: Part C, 2009, Vol.15, 1.

29 Z Xiong, YN Yan, RJ Zhang et al. Organism manufacturing engineering based on rapid prototyping principles, Rapid Prototyping Journal, 11(3): 160-166, 2005.

30. YN Yan, RJ Zhang, F Lin, Research and application on bio-manufacturing, in Proceedings on International Conference on Advanced Research in Virtual and Rapid Prototyping, eds. Paulo J. Bartolo et al., Publ. by Escola Superior de Technologia e Gestao de Leiria, Leiria, Portugal, pp 23-30, Oct. 1-4, 2003.

31. L Liu, Z Xiong, YN Yan, RJ Zhang et al. Multi-nozzle low-temperature deposition system for construction of gradient tissue engineering scaffolds. J. Biomedical Materials Research Part B-Applied Biomaterials, 88B (1): 254-263, 2009.

32. HX Liu, YN Yan et al. Preliminary results of direct cell-matrix assembly technology. Chinese Science Bulletin, 50(8): 830-832, 2005.

33. T Zhang et al. Channelled scaffolds for engineering myocardium with mechanical stimulation. J. Tissue Engineering and Regenerative Medicine, Nov 14th, DOI: 10.1002/term.481. [Epub ahead of print], 2011. PMID: 22081518.2011.

34. TS Wang, RJ Zhang and YN Yan. Preparation of bioactive hydroxyapatite on pure titanium. J. Bioactive and Compatible Polymers, 24(5): 169, 2009.

35. GX Tang, RJ Zhang et al. The effect of micro-arc oxidation time on the structure of the porous titania films prepared by a composite oxidation, Rare Metal Materials and Engineering, 34 (5): 821-825, 2005.

36. GX Tang, RJ Zhang et al. Preparation of anatase titanium film. Materials Letters, 58(12-13): 1857-1860, 2004.

37. R Yao, RJ Zhang et al. Design and evaluation of a cell microencapsulating device for cell assembly technology. J. Bioactive and Compatible Polymers, 24(5): 48, 2009.

38. R Yao, RJ Zhang et al. In Vitro angiogenesis of 3D tissue engineered adipose tissue. J. Bioactive and Compatible Polymers, 24(1): 5, 2009.

39. HT Gao et al. Data processing technology in rapid prototyping system. In YN Yan ed, Proceedings of the 2nd international conference on rapid prototyping & manufacturing 2002, Beijing, China, pp125-130, Beijing, China, August 19-20, 2002.

40. J Xu et al. The importance of software interface in RP technology. In YN Yan ed, Proceedings of the 2nd international conference on rapid prototyping & manufacturing 2002, Beijing, China, pp131-135, Beijing, China, August 19-20, 2002.

41. S Wang et al. Contour tracing in surface reconstruction. in YN Yan eds. Progress in rapid prototyping manufacturing and rapid tooling, Proceedings of the 1st international conference on rapid prototyping & manufacturing '98, Beijing, China, pp218-220, July 21-23, 1998.

42. SJ Li et al. Direct fabrication of a hybrid cell/hydrogel construct by a double-nozzle assembling technology. J. Bioactive and Compatible Polymers, 24: 249, 2009.

43. YN Yan et al. Direct construction of a three-dimensional structure with cells and hydrogel. J. Bioactive Compatible Polymers, 20(3): 259-269, 2005.

44. L Liu, Z Xiong, RJ Zhang et al. A novel osteochondral scaffold fabricated via multi-nozzle low-temperature deposition manufacturing. J. Bioactive and Competble Polymers, 24(S1): 18-30, 2009.

45. WG Zheng. Modeling and fabricating tissue engineering scaffolds with gradient structure. Ph.D. dissertation, Tsinghua University, Beijing, China, April 2003. (in Chinese)

46. WG Zeng et al. Modeling and designing gradient tissue engineering scaffolds with heterogenerous materials. In YN Yan ed, Proceedings of the 2nd international conference on rapid prototyping & manufacturing 2002, Beijing, China, pp136-142, Beijing, China, August 19-20, 2002.

Acknowledgments

The authors would like to offer their grateful thanks to Prof. Yongnian Yan, the First Director of the Institute of Bio-manufacturing Engineering, Tsinghua, China, and Prof. Wei Sun, the Second Director of the Institute, for their contributions to our group.